

## RESPONSE TIME OF MR DAMPERS FOR SEISMIC SEMIACTIVE CONTROL: EXPERIMENTAL MEASURES AND POSSIBLE PREDICTION

N. Caterino<sup>1</sup> and M. Spizzuoco<sup>2</sup>

<sup>1</sup> Department of Technology, University of Napoli Parthenope, Centro Direzionale, isola C4, 80123  
Naples, Italy  
nicola.caterino@uniparthenope.it

<sup>2</sup> Department of Structural Engineering, University of Napoli Federico II, Via Claudio 21, 80100 Na-  
ples, Italy  
spizzuoc@unina.it

**Keywords:** Semi-Active Control; Magnetorheological Dampers; Control Delays; Response time.

**Abstract.** *A wide experimental activity on two prototype magnetorheological (MR) semi-active (SA) dampers manufactured in Germany was conducted during an Italian research project, and it was partially devoted to investigate their promptness in the response. The experimental campaign has been performed on two properly designed setup configurations, by considering two different behaviours for the tested MR devices: a 'passive' behaviour (i.e., by keeping constant the feeding current during the entire test), or a 'semi-active' one, by driving them through an energy-based control algorithm. The experimental analysis of the devices' response time is presented in detail: it is shown how the control delays are strongly dependent on the effectiveness of the electric part of the control hardware, generally being less than 10 ms if special care is paid in designing the whole control chain. On the base of the experimental results, simple relationships are proposed to be assumed for the prediction of the amount of delay to be expected when a given change of current is going to be commanded, as well as the probability distributions of such delays calculated by fitting statistical available data. These distributions can be helpful for taking into account, in a refined model of a semi-actively controlled structure, the probability of occurrence of expected delays and/or to calibrate the compensation techniques included in some SA control algorithms, aiming at reducing the harmful effects these unavoidable delays may cause on the control effectiveness in terms of structural response reduction.*

## 1 INTRODUCTION

In the last decade, variable dampers have been widely considered in the framework of the seismic protection of structures, to implement semi-active (SA) control strategy of earthquake induced vibrations as well as smart passive ones [1, 2]. SA structural control via magnetorheological (MR) dampers is one of the most promising emerging technologies. The effectiveness of a SA strategy for vibration control strongly depends on the operation velocity. Unavoidable delays are involved in the control chain, even if a careful design of the system may strongly reduce their incidence. Few papers in literature show response time analyses of such devices [3-8], highlighting the need to further investigate this aspect, so crucial for the overall effectiveness of the above innovative control strategy. Data presented in some references numbered above seem to strongly disagree, setting the response time of MR dampers in a quite wide range: the apparent inconsistency is due to the different concepts of response times adopted by researchers. Herein a detailed analysis of the time response of a SA MR damper is presented, starting from the results of a wide experimental campaign conducted at the Laboratory of the University of Naples (Italy) Federico II on two full-scale (identical) prototype semi-active MR dampers provided by the German company Maurer Söhne [9].

## 2 TESTING APPARATUS

This section presents a comprehensive description of the testing set-up for the characterization of the prototype SA MR dampers. The total length of each device is 595 mm with a stroke of  $\pm 25$  mm, the external diameter is 100 mm, the mass is about 16 kg, and a maximum force of about 30 kN can be developed along its longitudinal axis (without rising of bending, shear and torsional moment in the piston rod). A patented magnetic circuit, composed by 3 coils in series, can generate the magnetic field in the device. The internal circuit of the damper has the following properties: a resistance of  $3.34 \Omega$ , a reactance of  $-1.27 \Omega$ , an impedance (modulus) of  $3.57 \Omega$  and an inductance of 276 mH. The current  $i$  in the circuit is provided in the range 0~3 A by a specific power supply type BOP (Bipolar Power Supply) provided by Kepco Inc. (New York, USA), model 50-4M, maximum power output of 200 W, maximum input power of 450 W, power source-power sink capabilities in the range  $\pm 50$  V (voltage) and  $\pm 4$  A (current): it is commanded from a remote location through a voltage signal in the range 0~10V, with alternative operations as voltage driver or as current driver.

The MR dampers have been experimentally tested in two different configurations (Figure 1) of a self-balanced testing apparatus. The dynamic actuator utilized has a stroke of  $\pm 250$  mm and can apply horizontal dynamic load up to 1,200 kN in tension and 440 kN in compression in the frequency range 0~5 Hz. Its external cylinder is firmly connected to a rigid steel plate through four steel bars with a diameter of 24 mm each. The MR device piston is connected to the moving part of the actuator through the interposition of a 100 kN load cell. In the first configuration, the main body of the damper is firmly linked to another rigid steel plate through four steel tubes with an external diameter of 114.3 mm and a thickness of 8 mm.

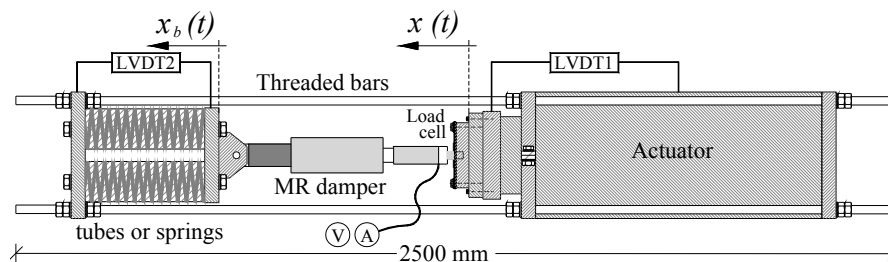


Figure 1: Schematic representation of the two experimental setups (with tubes and springs, respectively).

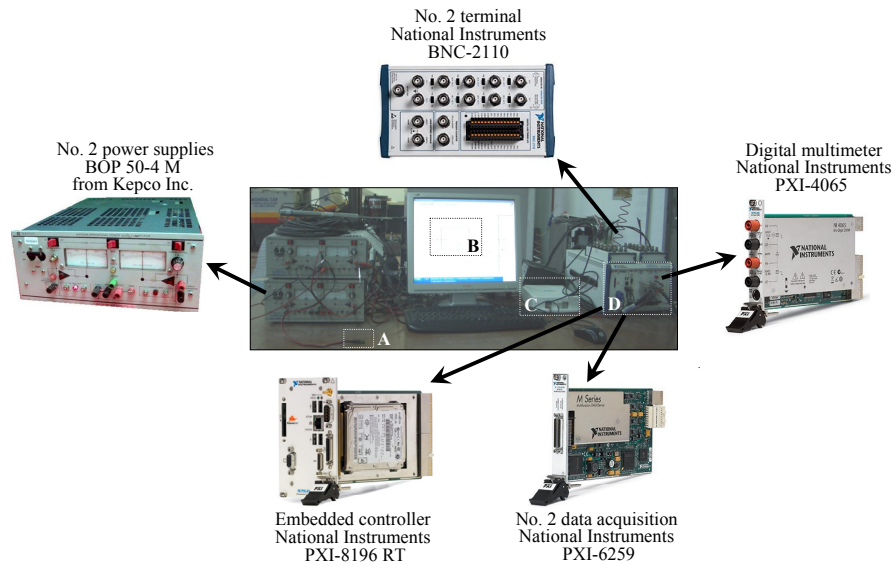


Figure 2: Main components of the electronic equipment adopted for the tests.

In the second configuration, the tubes are replaced by four elastic steel springs of stiffness 500 kN/m each, representing the elastic behaviour of an equivalent semi-active bracing system. An horizontal displacement transducer (“LVDT1” in Figure 1) was able to measure the displacement  $x$  of the actuator’s piston for the displacement control of its motion. In the second set-up configuration, an additional horizontal displacement transducer (“LVDT2”) with  $\pm 50$  mm stroke was mounted to measure the extension or compression  $x_b$  of the springs, that is, to indirectly evaluate the relative displacement of the damper ( $x_b - x$ ). The electronic equipment used for the tests is sketched in Figure 2.

### 3 EXPERIMENTAL ACTIVITY

Three groups of tests have been performed as listed in Table 1: they are labelled as ‘PA’ (‘passive’), ‘PR’ (‘promptness’) and ‘SA’ (‘semi-active’). Passive tests were addressed to investigate the dampers’ behaviour when fed by a constant intensity of current. Tests of promptness were designed and implemented to measure time delays involved in the SA control chain. Finally, for the semi-active tests, an energy based control algorithm [10] was applied to instantaneously select the optimal value of feeding current. Table 1 specifies:

- Displacements law imposed at the ends of the device. Harmonic, with frequency  $f$  in the range 0.5~3.0 Hz and amplitude  $d = 10\sim 20$  mm, or constant velocity type, with velocity  $v$  (0.1~0.3 m/s), amplitude  $d$  (10~20 mm) and 2 seconds pauses before inverting the sign of the velocity.
- Setup configuration, with steel tubes or springs (Figure 1).
- Control scheme adopted to drive the MR damper’s behaviour. In a voltage-driven scheme, the power supply provides a fixed voltage and the current slowly modifies until it reaches a value corresponding to the ratio voltage/resistance. In current-driven operations, the power supply provides a fast changing voltage spike so as to quickly modify the current inside the damper. Power supply having the capability of current-driven operation are referred to as ‘power source – power sink’.
- Algorithm adopted for promptness tests. The change of damper’s behaviour were commanded for each zero crossing of the displacement ( $x=0$ ) or velocity ( $\dot{x}=0$ ).

For the SA tests, the second above described setup configuration (with springs) has been adopted to simulate the semi-active operation of a dissipative bracing system installed on a

given structure. For these, the switch on of the damper has been commanded when the control force  $F$  and the relative velocity  $\dot{x}$  between the damper's ends had the same sign ( $F\dot{x} > 0$ ), the switch off in the contrary case ( $F\dot{x} \leq 0$ ). The SA brace simulated by the assembly MR damper plus elastic elements (springs) is able to temporarily store inside the springs the energy associated with their displacement during the time intervals when the power flowing into the SA assembly is positive, then to release it during fast-dissipation processes, imposed when the power flowing becomes negative. During these tests, the power supply has been used according to a current-driven scheme. All these tests have been also analyzed from a dissipated energy point of view in [11].

Group	No. of tests	Displacement law	Setup configuration	Power supply driven by	On/Off when
PA-1	60	harmonic	with tubes	Current	-
PA-2	60	constant velocity	with tubes	Current	-
PA-3	60	harmonic	with springs	Current	-
PR-1	12	harmonic	with tubes	Current	$\dot{x} = 0$
PR-2	12	harmonic	with tubes	Voltage	$\dot{x} = 0$
PR-3	9	harmonic	with tubes	Current	$\dot{x} = 0$
PR-4	20	constant velocity	with tubes	Current	$\dot{x} = 0$
PR-5	18	constant velocity	with springs	Current	$\dot{x} = 0$
SA-1	9	harmonic	with springs	Current	$F \cdot \dot{x} > 0$

Table 1: Main features of the tests performed.

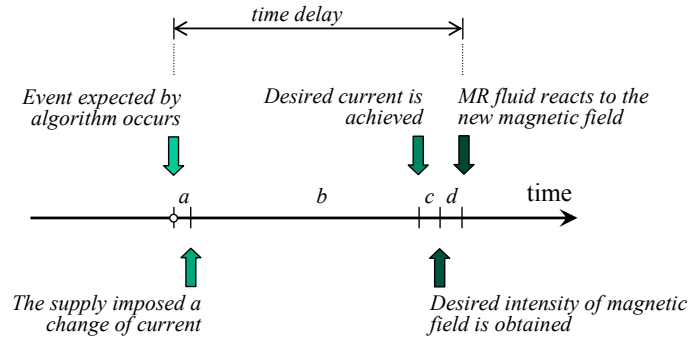


Figure 3: Schematic representation of time delays in a control chain involving MR dampers.

#### 4 PROMPTNESS OF THE PROTOTYPE SA MR DEVICES

The effectiveness of a SA strategy for vibration control strongly depends on the operation velocity. Unavoidable delays are involved in the control chain, even if their incidence may strongly be reduced through a careful design of the overall control system. The time response of a SA MR damper, depends on (Figure 3): *a*) the time needed by the power supply to impose a change of the current; *b*) the time needed to achieve the desired value of the current, according to the corresponding inductance; *c*) the time needed to achieve the corresponding value of the magnetic field; *d*) the time needed by the fluid to react to the change in the magnetic field. Item *b* generally plays the most significant role in the promptness of MR dampers. The time needed to modify the current, in particular, is strongly dependent on operations of the power supply. Figure 4 demonstrates that the time interval needed for the current to achieve the commanded value in the voltage-driven scheme results to be one order of magnitude larger than the one needed into a current-driven approach: from two harmonic tests performed at 1.0 Hz, 10 mm amplitude and 2 A maximum current intensity, belonging to groups PR-1 and PR-2 respectively, a time interval including two off→on and one on→off phases are extracted. The time windows report displacement, MR voltage, MR current and command

signal as given by the power supply. Part (a) of such figure refers to the current-driven scheme, part (b) to the voltage-driven approach. With reference to Figure 4a, it can be observed that when  $V_{com}$  goes from 0 to 5 V, after about 1 ms the voltage sent by the power supply to the damper reaches a spike of about 50 V which lasts about 6 ms, i.e. the time needed by the current to increase from zero to desired value; after this time, the voltage generated by the power supply falls down to the steady-state value of about 8 V. Similarly, when  $V_{com}$  varies from 5 to 0 V, after about 1 ms the voltage generated by the power supply jumps to -50 V and is kept constant for about 4 ms, that is the time needed until the current goes from 2 A to 0 A; after that, the voltage provided by the power supply is kept at a constant value of 0 V. In the voltage-driven operations (Figure 4b) when  $V_{com}$  goes from 0 to 1.5 V, the voltage  $V$  given by the power supply to the damper instantaneously varies from 0 to approximately 8 V, whereas the current  $i$  slowly increases from 0 to 2 A, due to the electric inductance of the coils inside the damper, taking about 215 ms to reach 95% of the final value. Similarly, the time needed by the current in an on→off switch is somewhat longer than 220 ms. It is worth to note that in case of voltage-driven operation the requirement of the power supply is about 16 W, but it increases to approximately 100 W in case of current-driven operation. This larger requirement allows to reduce the electrical response time of a SA MR damper of more than a order of magnitude (215 to 5 ms).

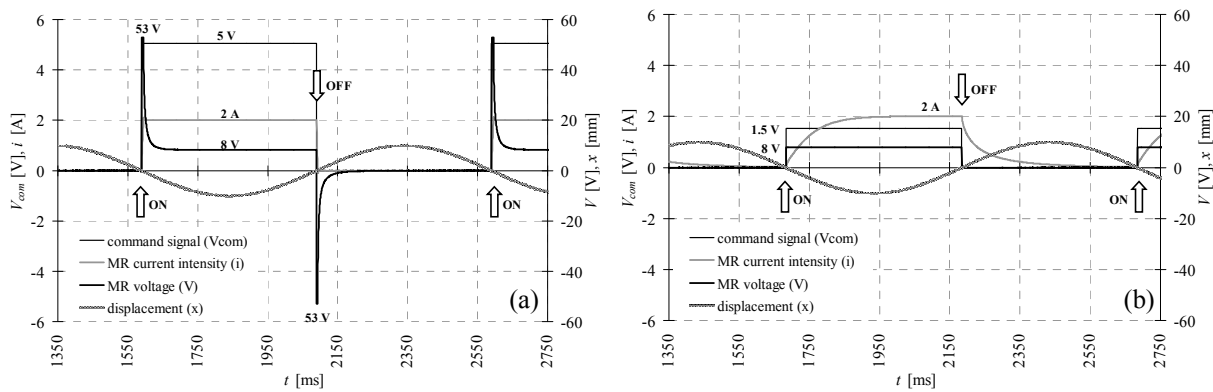


Figure 4: Some details of two tests of promptness. Current- (a) and voltage-driven (b) schemes.

Although the classification of the control delays described above (a to d) is based on a conceptual description, the testing apparatus was able to measure the response time of MR dampers as the sum  $\tau = \tau_a + \tau_c + \tau_e + \tau_m$ , where: (i)  $\tau_a$  is the time delay of the control electronics (i.e. the time interval starting when the switching algorithm recognizes that a given condition has occurred and ending when the CPU issues a command signal to the power supply); (ii)  $\tau_c$  is the time interval starting when the driving signal (in output from the algorithm) is issued to the power supply and ending when the current (in output from the power supply and in input to the device) begins to change; (iii)  $\tau_e$  is the time delay of the electrical part of the damper, which is the time interval starting when the current (into the device) begins to change and ending when the current reaches the commanded nominal value within a  $\pm 5\%$  tolerance; (iv)  $\tau_m$  is related to the mechanical part of the damper, representing the time interval between the instant when the current reaches its nominal value and the instant when the damper begins to react.

Figure 5 shows how the values of the electrical switch off delay measured during two types of harmonic tests (at 1.0 and 1.5 Hz, and 10 mm amplitude, groups PR-1 and PR-2) change according to the maximum value of feeding current  $i_{max}$  (1, 2 and 3 A).

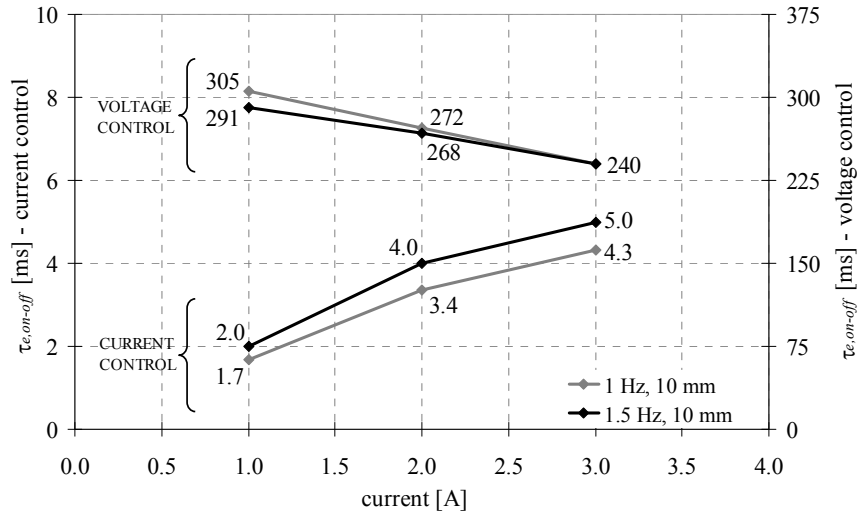


Figure 5: Amount of electrical switch off delay for harmonic displacement tests, as a function of the current.

Figure 6, which presents a time window of 200 ms extracted by three constant velocity tests of group PR-4 (at 0.2 m/s and 20 mm amplitude), shows 3 on→off (a) and 3 off→on phases (b), demonstrates that, when the current-driven approach was adopted, the time needed to the MR damper's force to get the final desired value resulted to be almost the same (about 30 ms) for each investigated maximum value of current intensity.

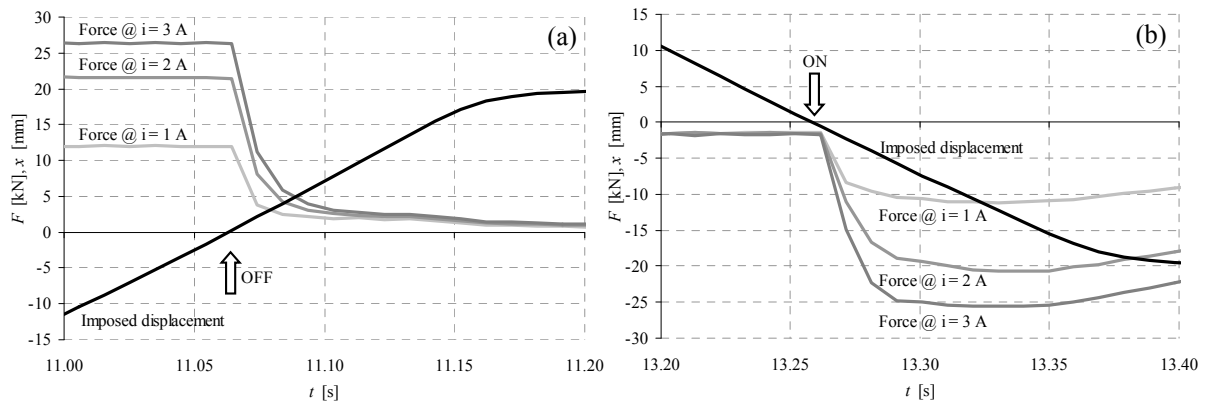


Figure 6: Constant velocity tests at 0.2 m/s, 20 mm. Decay (a) and rising (b) of the MR force when a switch off and a switch on are given respectively (current-driven approach).

The response times  $\tau_a$ ,  $\tau_c$ ,  $\tau_e$ ,  $\tau_m$  have been measured at two on→off and two off→on phases for each of all performed tests. A total of 120 experimental values for each of them have been measured in the case of the current-driven scheme, 24 in that of the voltage-driven scheme. Time delays  $\tau_a$  and  $\tau_c$  turned out to assume a rather stable value equal to 0.4 ms for both the on→off and the off→on phases, resulting to be practically independent from the maximum commanded current. The mechanical response time  $\tau_m$ , measured in both the switch off and switch on phases, resulted in an almost stable value, on average equal to 1 ms. Conversely, as expected, electrical delays  $\tau_e$  resulted to be strongly dependent on the level of current intensity as well as on the adopted scheme (voltage- or current-driven) adopted to control MR damper's behavior. All the measured  $\tau_e$  values are graphically reported in Figure 7, where those referred to a switch on are indicated by gray dots, those to a switch off by black dots. Parts (a) and (b) of such figure refer to the current-driven and voltage-driven approaches respectively. When the current-driven operations have been imposed,  $\tau_e$  turned out to be in the

interval 2~6 ms for the on→off switches, 2~9 ms for the off→on phases. Results of the tests performed according to the voltage-driven scheme resulted to be included in the intervals 230~300 ms and 125~250 ms for cases of switch-on and switch off respectively. Regression lines and their equations (see Figure 7) may further help the reader in interpreting the trend of these data as a function of the current intensity. These equations can also be included in the numerical model of a semi-actively protected structures when control delays have to be explicitly accounted for.

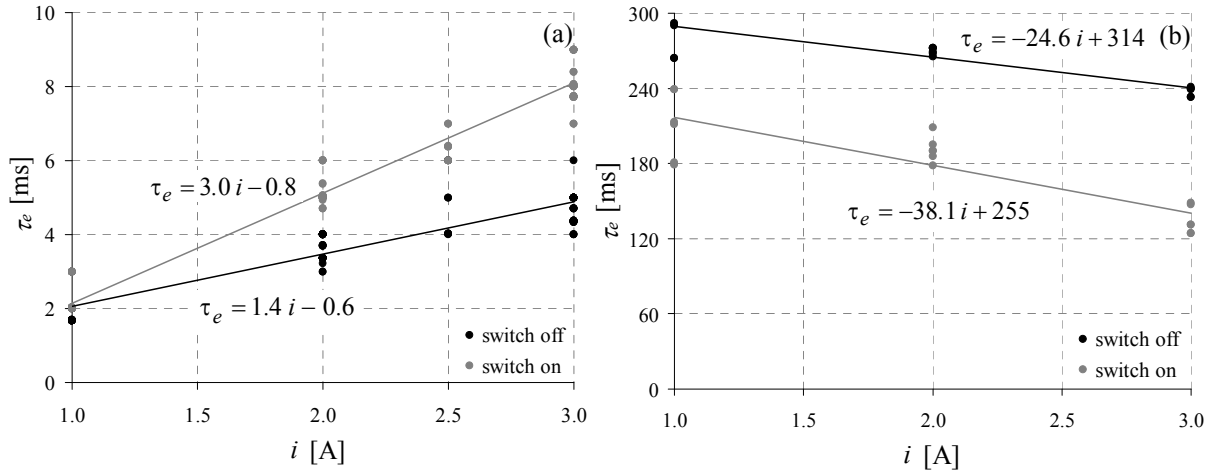


Figure 7: Summary of all the measured  $\tau_e$  time delays: current-driven (a) and voltage-driven (b) approaches.

The experimental measures of  $\tau_e$  at on→off switches ( $\tau_{e,off}$ ) have been statistically analyzed by dividing each of them by the maximum feeding current  $i$  of the corresponding test, and by singling out 8 classes of values of the normalized delay  $\tau_{e,off}/i$ , from zero to 4.0 ms/A (each class has an amplitude of 0.5 ms/A). The relative frequency density has been calculated for each class as the ratio of the relative frequency over the amplitude of the class, being the relative frequency of a class the number of measures of  $\tau_{e,off}/i$  belonging to it, normalized by the total number of measurements. The same operation has been done also with reference to the values of  $\tau_e$  measured for off→on cases ( $\tau_{e,on}$ ).

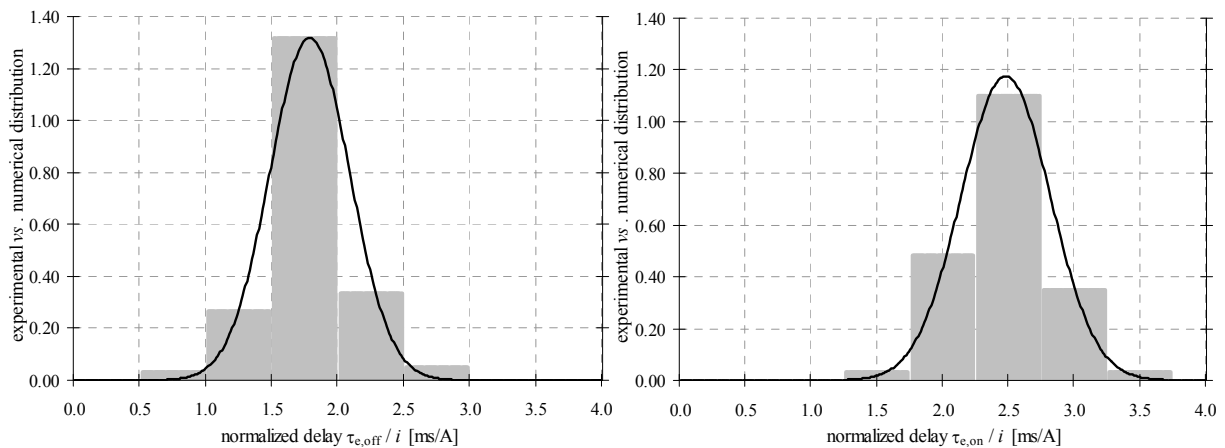


Figure 8: Statistical analysis of the values  $\tau_e$  normalized by the current intensity. Fitting probability distributions.

The calculated densities correspond to the grey histograms of Figure 8, where the black curve fits the experimental data according to a Gaussian distribution function of variable  $x$ , measuring the electrical delay  $\tau_e$  normalized by the current intensity, with mean  $\mu$  (1.786

ms/A for  $\tau_{e,off}$ , 2.478 ms/A for  $\tau_{e,on}$ ) and standard deviation  $\sigma$  (0.303 ms/A for  $\tau_{e,off}$ , 0.339 ms/A for  $\tau_{e,on}$ ). These distributions can be helpful to predict the amount of delays associated to the SA control of a given structure equipped with the examined MR dampers, taking into account the probability they actually may occur during a seismic excitation.

## 5 CONCLUSIONS

The promptness of semi-active MR devices turned out to be almost exclusively dependent on the effectiveness of the electric part of the control hardware. Rheology and nature of MR fluids seem to play a negligible role on the response time of SA MR devices, while it is necessary a careful design of the electric part and of the power supply. The adoption of current-driven operations is practically mandatory. Provided that an adequate electric hardware be available and properly tuned, the experimental activity at the base of this paper demonstrated that the response time of a SA MR dampers can be comfortably bounded to 8~10 ms. In this case, the measured operating delay of such dampers is mainly associated to the time needed by the current to form the magnetic field in which the fluid is immersed and, in turn, to the design of the coils. In many practical applications, a time interval of 8~10 ms interval can be considered really short, and thus almost negligible, for example compared to typical periods of vibration of civil structures. The present paper proposes simple relationships useful to predict the amount of delay to be expected when a given change of current is going to be commanded, as well as it shows the probability distributions of such delays calculated by fitting statistical available data. The latters can be useful to be involved in the compensation schemes some SA control algorithms include, aiming at reducing the harmful effects of these unavoidable delays on the effectiveness of control systems.

A similar analysis is in progress with reference to data available from shaking table tests of a steel frame structure [12] equipped with the same two prototype devices herein discussed.

## REFERENCES

- [1] G. Maddaloni, N. Caterino, A. Occhiuzzi, Semi-active control of the benchmark highway bridge based on seismic early warning systems. *Bulletin of Earthquake Engineering*, **9** (5), 1703-1715, 2011. doi:10.1007/s10518-011-9259-1
- [2] G. Maddaloni, N. Caterino, G. Nestovito, A. Occhiuzzi, Use of seismic early warning information to calibrate variable dampers for structural control of a highway bridge: evaluation of the system robustness. *Bulletin of Earthquake Engineering*. (in press)
- [3] G. Yang, B.F. Spencer, J.D. Carlson, M.K. Sain, Large-scale MR fluid dampers: modeling and dynamic performance considerations. *Engineering Structures*, **24**, 309-323, 2002.
- [4] A. Milecki, Investigation and control of magneto-rheological fluid dampers. *Intl. Jour. Mach. Tools & Manuf.*, **41**, 379-391, 2001.
- [5] J.H. Koo, F.D. Goncalves, M. Ahmadian, A comprehensive analysis of the response time of MR dampers. *Smart Mater. Struct.*, **15**, 351-358, 2006
- [6] A. Occhiuzzi, M. Spizzuoco, G. Serino, Experimental analysis of magnetorheological dampers for structural control. *Smart Materials and Structures*, **12**, 703-711, 2003.
- [7] L. Yang, D.F. Fubin, A. Eriksson, Analysis of the optimal design strategy of a magnetorheological smart structure. *Smart Material and Structures*, **17**, 8 pp, 2008.



- [8] X. Guan, P. Guo, J. Ou, Study of the response time of MR dampers. *2<sup>nd</sup> International Conference on Smart Materials and Nanotechnology in Engineering*, Proceedings of SPIE 7493, 2009.
- [9] N. Caterino, M. Spizzuoco, A. Occhiuzzi, Understanding and modelling the physical behaviour of magnetorheological dampers for seismic structural control. *Smart Materials and Structures*, **20** 065013 doi: 10.1088/0964-1726/20/6/065013, 2011.
- [10] A. Occhiuzzi, M. Spizzuoco, Experimental analysis of a semi-actively controlled steel building. *Structural Engineering and Mechanics*, **19** (6), 721-747, 2005.
- [11] N. Caterino, M. Spizzuoco, A. Occhiuzzi, Promptness and dissipative capacity of MR dampers: experimental investigations. *Structural Control and Health Monitoring*, 2013 (in press).
- [12] N. Caterino, M. Spizzuoco, A. Occhiuzzi A, Experimental comparison of control algorithms for systems based on SA MR dampers for seismic response reduction. *Smart Structures and Systems*. (in press)